Quantum magneto-optics of graphite with trigonal warping

L. A. Falkovsky
L.D. Landau Institute for Theoretical Physics, Moscow 119334, Russia and
Institute of the High Pressure Physics, Troitsk 142190, Russia
(Received 17 June 2011; published 13 September 2011)

The optical conductivity of graphite in quantizing magnetic fields is studied. Both the dynamical conductivities, longitudinal as well as Hall's, are analytically evaluated. The conductivity peaks are explained in terms of electron transitions. We have shown that the trigonal warping in graphite can be considered within the perturbation theory at strong magnetic fields larger than approximately 1 T. The main optical transitions obey the selection rule with $\Delta n = 1$ for the Landau number n, however, the $\Delta n = 2$ transitions due to the trigonal warping with small probability are also essential. The Kerr rotation and reflectivity in graphite in the quantizing magnetic fields are calculated. Parameters of the Slonczewski-Weiss-McClure model are used in the fit taking into account the previous dHvA measurements and correcting some of them for the case of strong magnetic fields.

DOI: 10.1103/PhysRevB.84.115414 PACS number(s): 76.40.+b, 78.20.−e, 81.05.uf

I. INTRODUCTION

Properties of graphite have attracted much attention for more than 50 years. Many of that properties were successfully explained within the Slonczewski-Weiss-McClure (SWMC) theory.[1] The most accurate method to study the band structure of graphite is a study of the Landau levels (LLs) through experiments such as magneto-optics[2–10] and magneto-transport.[11–15] However, the interpretation of the experimental results involves a significant degree of uncertainty since, as it is not clear how the resonances should be identified and which electron transitions they correspond to.

The SWMC theory requires the use of many tight-binding parameters and provides the simple description of observed phenomena either in the semiclassical limit of week magnetic fields or for high frequencies when the largest tight-binding interlayer parameter γ_1 plays the leading role.[16] It is more difficult to take into account the parameter γ_3 known as "trigonal warping." Usually, it is either neglected[9,16–19] or considered numerically.[20–24] The Bohr-Sommerfeld quantization condition was applied in Ref. 25 to find in low magnetic fields the level structure including the trigonal warping. In any case, only the problem of levels was considered so far, and no calculations of conductivities were done in order to evaluate the optic properties of graphite. The problem appearing for three-dimensional systems in the magnetic field connects partly with integrating over the momentum projection k_z along the magnetic field.

The SWMC model can be simplified assuming that only the integration limits such as the K and H points in the brillouin zone produce the main contributions.[8,17,18] Such an approximation is similar to the theory of magneto-optical effects in topological insulators[26] and graphene.[27] However, the band extrema or the integration limits at the Fermi level can also contribute into the absorption. Therefore, the analytical expression for the dynamic conductivity in the presence of magnetic fields is needed for the interpretation of the magneto-optics experiments.

In this paper, motivated by the experimental study of the Faraday rotation in single- and multilayer graphene,[10] we propose a theory of magneto-optics phenomena in graphite in strong magnetic fields including the interlayer hopping parameters γ_3 and γ_4 in the Hamiltonian. The trigonal warping γ_3 is considered as a perturbation with the help of the Green's function method. Not only the energy-level structure corrected due to the trigonal warping is found, but the expressions for the longitudinal and Hall dynamical conductivities are derived. Our main theoretical finding is the reflectivity and the Kerr angle for graphite in strong magnetic fields.

II. LANDAU LEVELS IN GRAPHITE WITH TRIGONAL WARPING

Taking into account the tight-binding parameters of the SWMC theory, the effective Hamiltonian near the KH line of the brillouin zone in graphite writes in the form of Refs. 22 and 23:

$$H(\mathbf{k}) = \begin{pmatrix} \tilde\gamma_5 & vk_+ & \tilde\gamma_1 & \tilde\gamma_4 vk_-/\gamma_0 \\ vk_- & \tilde\gamma_2 & \tilde\gamma_4 vk_-/\gamma_0 & \tilde\gamma_3 vk_+/\gamma_0 \\ \tilde\gamma_1 & \tilde\gamma_4 vk_+/\gamma_0 & \tilde\gamma_5 & vk_- \\ \tilde\gamma_4 vk_+/\gamma_0 & \tilde\gamma_3 vk_-/\gamma_0 & vk_+ & \tilde\gamma_2 \end{pmatrix}, \tag{1}$$

where $k_\pm = \mp ik_x - k_y$ are the momentum components and v is the velocity parameter in the intralayer directions; $\tilde\gamma_j$ are the functions of the k_z momentum in the main axis direction,

$$\tilde\gamma_2 = 2\gamma_2 \cos(2k_z d_0), \quad \tilde\gamma_5 = 2\gamma_5 \cos(2k_z d_0) + \Delta,$$
$$\tilde\gamma_i = 2\gamma_i \cos(k_z d_0) \quad \text{for} \quad i = 1,3,4,$$

with the distance $d_0 = 3.35$ Å between the layers in graphite. The nearest-neighbor hopping integral $\gamma_0 \approx 3$ eV corresponds with the in-layer interatomic distance $a_0 = 1.415$ Å and the Fermi velocity parameter $v = 1.5a_0\gamma_0 = 10^6$ m/s.

For the zero magnetic field, the eigenvalues of the Hamiltonian give four close bands. In the magnetic field B, the momentum projections $k_{x,y}$ become the operators obeying the commutation rule $\{\hat k_+, \hat k_-\} = -2e\hbar B/c$, and we use the relations,

$$\hat k_+ = \sqrt{2|e|\hbar B/c}\, a, \quad \hat k_- = \sqrt{2|e|\hbar B/c}\, a^+,$$

involving the creation a^+ and annihilation operators a. We will write only one of two x, y space coordinates including the

corresponding degeneracy proportional to the magnetic field in the final results.

We search the eigenfunction of the Hamiltonian (1) in the form,

$$\psi_{sn}^{\alpha}(x) = \begin{cases} C_{sn}^{1}\varphi_{n-1}(x) \\ C_{sn}^{2}\varphi_{n}(x) \\ C_{sn}^{3}\varphi_{n-1}(x) \\ C_{sn}^{4}\varphi_{n-2}(x) \end{cases}, \tag{2}$$

where $\varphi_n(x)$ are orthonormal Hermitian functions with the Landau numbers $n \geqslant 0$. One sees that every row in the Hamiltonian (1) becomes proportional to the definite Hermitian function if the terms with γ_3 are omitting. We will show that the terms proportional to γ_3/γ_0 can be considered within the perturbation theory at strong magnetic fields.

Canceling the Hermitian functions from the equations, we obtain a system of the linear equations for the eigenvector $\mathbf{C}_{sn}$,

$$\begin{pmatrix} \tilde{\gamma}_5-\varepsilon & \omega_c\sqrt{n} & \tilde{\gamma}_1 & \omega_4\sqrt{n-1} \\ \omega_c\sqrt{n} & \tilde{\gamma}_2-\varepsilon & \omega_4\sqrt{n} & 0 \\ \tilde{\gamma}_1 & \omega_4\sqrt{n} & \tilde{\gamma}_5-\varepsilon & \omega_c\sqrt{n-1} \\ \omega_4\sqrt{n-1} & 0 & \omega_c\sqrt{n-1} & \tilde{\gamma}_2-\varepsilon \end{pmatrix} \times \begin{Bmatrix} C_{sn}^{1} \\ C_{sn}^{2} \\ C_{sn}^{3} \\ C_{sn}^{4} \end{Bmatrix} = 0, \tag{3}$$

where the band number $s = 1,2,3,4$ numerates the solutions at given n from the bottom, $\omega_c = v\sqrt{2|e|\hbar B/c}$ and $\omega_4 = \tilde{\gamma}_4\omega_c/\gamma_0$.

The eigenvalues of the matrix in Eq. (3) are easily found; they are shown in Fig. 1 as a function of the momentum k_z. For each Landau number $n \geqslant 2$ and momentum k_z, there are four eigenvalues $\varepsilon_s(n)$ and four corresponding eigenvectors, Eq. (2),

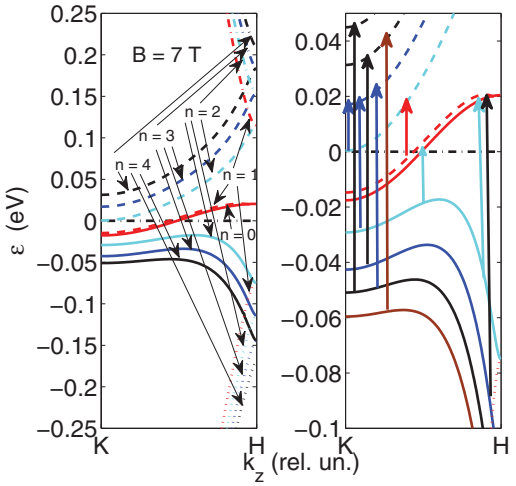

FIG. 1. (Color online) LLs ε_{sn} for $n =$ 0–4 in four bands $s = 1,2,3,4$ (in dotted, solid, dashed, and dash-dotted lines, correspondingly) as functions of momentum k_z along the KH line in the brillouin zone ($K = 0$, $H = \pi/2d_0$) at the magnetic field $B =$ 7 T with the SWMC model parameters given in Table I. The main electron transitions shown in the right panel below 100 meV are possible between the levels with the selection rule $\Delta n = \pm 1$; see text.

marked by the band subscript s. We will use the notation $|sn\rangle$ for levels. In addition, there are four levels. One of them,

$$\varepsilon_1(n=0) = \tilde{\gamma}_2, \tag{4}$$

for $n = 0$ with the eigenvector $\mathbf{C}_0 = (0,1,0,0)$ as is evident from Eq. (2). It intersects the Fermi level and belongs to the electron (hole) band near the K (H) point. The other three levels indicated with $n = 1$ and $s = 1,2,3$ are determined by the first three equations of the system (3) with $C_{s1}^{4} = 0$.

The $|21\rangle$ level is close to the $|10\rangle$ level. In the region of k_z, $\gamma_1/\cos z \gg \gamma_2$, where the electrons are located, this level has the energy,

$$\varepsilon_2(n=1) = \tilde{\gamma}_2 - 2\frac{\omega_c^2\tilde{\gamma}_4}{\tilde{\gamma}_1\gamma_0}.$$

In the same region, the two closest bands ($s = 2,3$) with $n \geqslant 2$ are written as

$$\varepsilon_{2,3}(n) = \tilde{\gamma}_2 - \frac{\omega_c^2\tilde{\gamma}_4}{\tilde{\gamma}_1\gamma_0}(2n-1) \mp \frac{\omega_c^2}{\tilde{\gamma}_1}\sqrt{n(n-1)}, \tag{5}$$

within accuracy of $(\tilde{\gamma}_4/\gamma_0)^2$.

A simplest way to evaluate the corrections resulting from the warping γ_3 consists in the consideration of the relative Green's function having the poles at the electron levels. The corrections to the levels can be found in the iterations,

$$\mathbf{G}_{m+1}(x,x') = \int dx''\mathbf{G}_0(x,x'')\mathbf{V}(x'')\mathbf{G}_m(x'',x'), \tag{6}$$

where $\mathbf{V}(\mathbf{x})$ has only two matrix elements $V^{42} = \omega_c\tilde{\gamma}_3 a^{+}/\gamma_0$ and $V^{24} = V^{42*}$ in the Hamiltonian (1). The Green's function of the unperturbed Hamiltonian writes

$$G_0^{\alpha\beta}(\varepsilon,x,x') = \sum_{sn}\frac{\psi_{sn}^{\alpha}(x)\psi_{sn}^{*\beta}(x')}{\varepsilon-\varepsilon_{sn}}. \tag{7}$$

In the second iteration, we get the corrections,

$$\int dx_1dx_2G_0^{\alpha4}(x,x_1)V^{42}(x_1)G_0^{22}(x_1,x_2)V^{24}(x_2)G_0^{4\beta}(x_2,x'),$$

and the similar term with the substitution of the superscripts $2 \leftrightarrow 4$. The matrix elements of the perturbation V are easily calculated with respect to the Hermitian functions of Eqs. (7) and (2) and we obtain for the diagram shown in the upper part of Fig. 2,

$$\left(\frac{\omega_c\tilde{\gamma}_3}{\gamma_0}\right)^2\sum_{s'sn}\frac{(n-2)\left|C_{sn}^{4}C_{s',n-3}^{2}\right|^2\psi_{sn}^{\alpha}(x)\psi_{sn}^{*\beta}(x')}{(\varepsilon-\varepsilon_{sn})(\varepsilon-\varepsilon_{s',n-3})(\varepsilon-\varepsilon_{sn})}. \tag{8}$$

This correction plays an important role near the poles of the Green's function. Therefore, we can substitute ε_{sn} instead of ε in the second factor of the denominator and represent this correction as a shift $\delta\varepsilon_{sn}$ of the poles $(\varepsilon-\varepsilon_{sn}-\delta\varepsilon_{sn})^{-1}$ with

$$\delta\varepsilon_s(n) = \left(\frac{\omega_c\tilde{\gamma}_3}{\gamma_0}\right)^2\sum_{s'}\left\{\frac{(n-2)\left|C_{sn}^{4}C_{s',n-3}^{2}\right|^2}{\varepsilon_s(n)-\varepsilon_{s'}(n-3)} + \frac{(n+1)\left|C_{sn}^{2}C_{s',n+3}^{4}\right|^2}{\varepsilon_s(n)-\varepsilon_{s'}(n+3)}\right\}, \tag{9}$$

where the first term should be omitted for $n-3<0$. In fact, our illustration is nothing but a calculation of the electron

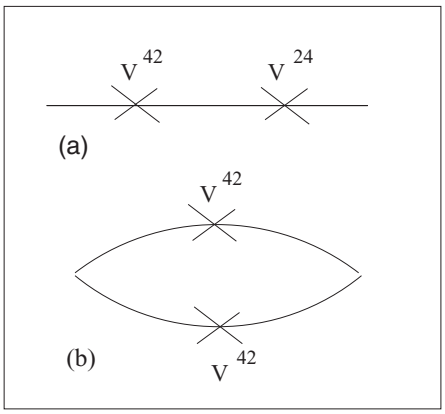

FIG. 2. Diagrams for the second iteration of the perturbation theory; corrections to the Green's function (a) and corrections to the vertex in conductivity (b).

self-energy and the naive expansion of the denominator can be indeed replaced by summarizing of the corresponding diagrams.

Comparing the corrections, Eq. (9), with the main contribution Eq. (5), we find that the perturbation theory is valid when an expansion parameter $(\tilde{\gamma}_3\tilde{\gamma}_1/\gamma_0\omega_c)^2$ becomes small (i.e., for the strong magnetic fields $B > 1$ T). The corrected $|10\rangle$ level writes

$$\varepsilon_1(n=0) = \tilde{\gamma}_2 + \left(\frac{\omega_c\tilde{\gamma}_3}{\gamma_0}\right)^2 \sum_{s'} \frac{|C^4_{s'3}|^2}{\tilde{\gamma}_2 - \varepsilon_{s'}(3)}. \tag{10}$$

The $|21\rangle$ level is very close to the level with $n = 0$ [Eqs. (4) and (10)].

Our expressions for the levels with the corrections (9) and (10) give the same results as obtained in Ref. 21 by the numerical method of truncating the infinite matrix.

III. CONDUCTIVITIES IN MAGNETIC FIELDS

In the collisionless limit when the relaxation rate Γ is much less than the frequency, $\Gamma \ll \omega$, the conductivity is expressed in terms of the correlation function

$$\mathcal{P}(\omega) = T\sum_{\omega_m}\int dx dx' \mathrm{Tr}\{v^i G(\omega_+,x,x')v^j G(\omega_-,x',x)\}, \tag{11}$$

where we should (i) summarize over Matsubara's frequencies ω_m, (ii) take the trace over the Landau and band numbers, (iii) make an analytic continuation into real frequencies ω, and (iiii) substrate from the result its value at $\omega = 0$ (for details see Refs. 28 and 29).

The velocity matrices v^i in Eq. (11) are given by the derivative of the Hamiltonian, Eq. (1),

$$\mathbf{v} = \frac{\partial H(\mathbf{k})}{\partial \mathbf{k}}. \tag{12}$$

First we consider the largest velocity operators, Eq. (12), which do not involve the parameter $\tilde{\gamma}_3/\gamma_0$. Straightforward calculations yield two independent components of the dynamical conductivity,

$$\left.\begin{matrix}\sigma_{xx}(\omega)\\ i\sigma_{xy}(\omega)\end{matrix}\right\} = i\sigma_0\frac{4\omega_c^2}{\pi^2}\sum_{n,s,s'}\int_0^{\pi/2} dz \frac{\Delta f_{ss'n}}{\Delta ss'n}|d_{ss'n}|^2 \times [(\omega + i\Gamma + \Delta_{ss'n})^{-1} \pm (\omega + i\Gamma - \Delta_{ss'n})^{-1}], \tag{13}$$

where $\Delta_{ss'n} = \varepsilon_{sn} - \varepsilon_{s',n+1}$ is the level spacing including the corrections given in Eqs. (9) and (10), $\Delta f_{ss'n} = f(\varepsilon_{s'n+1}) - f(\varepsilon_{sn})$ is the difference of the corresponding Fermi-Dirac functions, and

$$d_{ss'n} = C^2_{sn}C^1_{s'n+1} + C^3_{sn}C^4_{s'n+1} + (\tilde{\gamma}_4/\gamma_0)\left(C^1_{sn}C^4_{s'n+1} + C^2_{sn}C^3_{s'n+1}\right) \tag{14}$$

is the dipole matrix element. These electron transitions obey the selection rule,

$$\Delta n = 1,$$

and will be referenced as the strong lines. The integration over the brillouin half-zone, $0 < z < \pi/2$, and the summation over the Landau number n as well as the bands s,s' should be done in Eq. (13). The conductivity units,

$$\sigma_0 = \frac{e^2}{4\hbar d_0},$$

have a simple meaning, being the graphene dynamic conductivity[30] $e^2/4\hbar$ multiplied by the number $1/d_0$ of layers within the distance unit in the main axis direction.

Now we consider the terms with $\tilde{\gamma}_3/\gamma_0$ in the velocity operators [Eq. (12)]. Calculating the correlation function Eq. (11) we get an additional term in the conductivity, which can be obtained from Eq. (13) with the substitutions,

$$n+1 \to n+2,$$

and with the matrix element,

$$d_{ss'n} = (\tilde{\gamma}_3/\gamma_0)C^2_{sn}C^4_{s'n+2},$$

instead of the matrix element given by Eq. (14). These transitions obey the selection rule,

$$\Delta n = 2,$$

and will be referenced as the weak lines. I should emphasize that Nakao[21] did not recognize the order of the perturbation theory in his numerical calculations and therefore all the terms with different Δn appear together.

So far we considered the γ_3 corrections to the Green's function (i.e., to the levels). These calculations are similar to the analysis of the electron self-energy in the problem of the interaction with defects (see, for instance, Ref. 28; pages 327–334). However, there are so-called vertex corrections to the self-energy shown at the bottom of Fig. 2. They result from the quartet of the coupled Landau levels, which interfere while the selection rules $\Delta n = 1$ and $\Delta n = 2$ are allowed. For compactness, let us denote this quartet of given n as the following:

$$a = |sn\rangle, \quad b = |s',n+1\rangle, \quad c = |s_1,n+3\rangle, \quad d = |s_1',n+4\rangle, \tag{15}$$

TABLE I. The parameters of the Hamiltonian, Eq. (1), their values in the SWMC model, and obtained in the experimental works, all in meV.

	γ_0	γ_1	γ_2	γ_3	γ_4	γ_5	Δ	ε_F
(1)	3050	360	−10.2	270	−150	−1.5	16	−4.1
S[a]	γ_0	γ_1	$2\gamma_2$	γ_3	$-\gamma_4$	$2\gamma_5$	$\Delta + 2(\gamma_2 - \gamma_5)$	$2\gamma_2 + \varepsilon_F$
M[b]	3160	390	−20	276	44	38	8	−24
D[c]	3120	380	−21	315	120	−3	−2	–

[a]SWMC, Reference 1.
[b]Mendez *et al.*, Reference 5.
[c]Doezema *et al.*, Reference 4.

where the band numbers s,s',s_1, and s_1' are arbitrary.

The corresponding corrections to conductivities write

$$\left.\begin{matrix}\delta\sigma_{xx}(\omega)\\ i\delta\sigma_{xy}(\omega)\end{matrix}\right\} = 2i\sigma_0 \sum_{nss's_1s_1'} \int_0^{\pi/2} dz \left(\frac{2\omega_c^2\tilde{\gamma}_3}{\pi\gamma_0}\right)^2 \times C_a^2C_b^2C_c^4C_d^4\left(C_b^1C_a^2 + C_a^3C_b^4\right)\left(C_d^1C_c^2 + C_c^3C_d^4\right) \times \sqrt{(n+1)(n+2)}(\varepsilon_b - \varepsilon_d)^{-1}(\varepsilon_a - \varepsilon_c)^{-1} \times \{[(\omega + i\Gamma + \varepsilon_b - \varepsilon_a)^{-1} \pm (\omega + i\Gamma - \varepsilon_b + \varepsilon_a)^{-1}]\partial_{ab} + [(\omega + i\Gamma + \varepsilon_b - \varepsilon_c)^{-1} \pm (\omega + i\Gamma - \varepsilon_b + \varepsilon_c)^{-1}]\partial_{cb} + [(\omega + i\Gamma + \varepsilon_d - \varepsilon_a)^{-1} \pm (\omega + i\Gamma - \varepsilon_d + \varepsilon_a)^{-1}]\partial_{ad} + [(\omega + i\Gamma + \varepsilon_d - \varepsilon_c)^{-1} \pm (\omega + i\Gamma - \varepsilon_d + \varepsilon_c)^{-1}]\partial_{cd}\}, \quad (16)$$

where

$$\partial_{ab} = [f(\varepsilon_a) - f(\varepsilon_b)]/(\varepsilon_b - \varepsilon_a),$$

and $f(\varepsilon_a)$ is the Fermi-Dirac function. The terms with the negative radicand should be omitted while summing over n and all band numbers from Eq. (15).

IV. HALL AND LONGITUDINAL CONDUCTIVITIES WITH THE SWMC PARAMETERS

The parameters of Eq. (1) used in the calculations are listed in Table I (see also Ref. 31). The hopping integrals γ_0 to γ_3 are close to the values determined in observations of the semiclassical ShdH effect. The Fermi energy equal to $\varepsilon_F = -4.1$ meV agrees at the zero magnetic field with the measurements of the extremal Fermi-surface cross sections and the masses of holes and electrons. Connections with the notation for the same parameters in the SWMC model are given in the "SWMC" line. The values of parameters γ_4, γ_5, and Δ determined in various experiments are very different, we use γ_5 and Δ obtained by Doezema *et al.*[4] (given in Table I in the "SWMC" notations) and take for γ_4 the approaching value. In the quantum limit, when electrons and holes occupy only $|10\rangle$ and $|21\rangle$ levels, the Fermi energy must cross these close levels at the middle of the KH line. It means that the Fermi level becomes higher at such, the magnetic fields taking the value $\varepsilon_F \approx -1$ meV.

The results of calculations are represented in Figs. 3–4. Let us emphasize that the imaginary part of the dynamical conductivity is of the order of the real part.

One can see in Fig. 3(a), that the longitudinal conductivity calculated per one graphite layer tends on average to the graphene universal conductance. The main contribution in the sharp 16-meV line is resulted from the electron $|21\rangle \to |32\rangle$ transitions (15 meV) about the K point where the $|32\rangle$ level coincides with the Fermi level (within accuracy of the width Γ or temperature T). Then, the transitions $|22\rangle \to |21\rangle$ produce the broad band. The low-frequency side of the band (23 meV, at the intersection of the $|21\rangle$ level with the Fermi level) contributes into the 16-meV line. In the same 16-meV line, the transitions $|32\rangle \to |33\rangle$ can contribute as well if the band $|32\rangle$ contains the electrons.

The next doublet at 43 meV arises from the transitions $|23\rangle \to |32\rangle$ and $|22\rangle \to |33\rangle$ at the K point. The 68-meV doublet splitting results due to the electron-hole asymmetry from the transitions $|24\rangle \to |33\rangle$ (65 meV) and $|23\rangle \to |34\rangle$ (69 meV) at the K point of the brillouin zone.

The 89-meV line is more complicated. First, there are the electron transitions $|24\rangle \to |35\rangle$ (89 meV) and $|25\rangle \to |34\rangle$

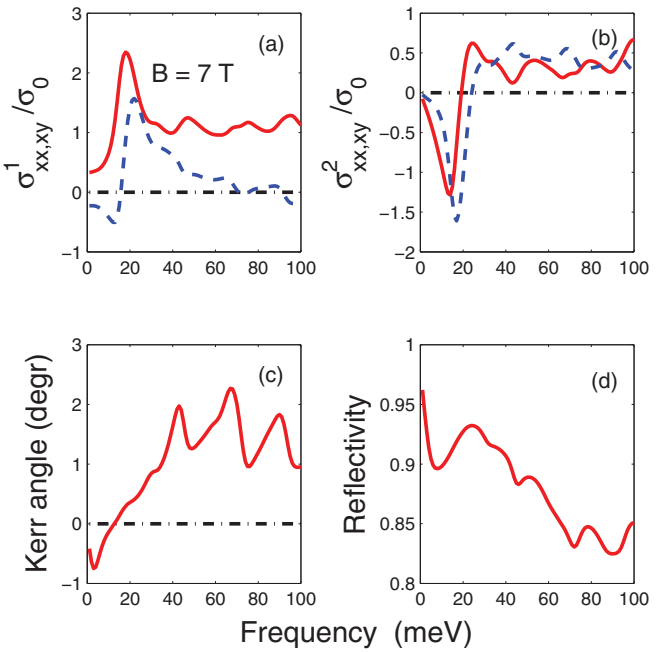

FIG. 3. (Color online) Real (a) and imaginary (b) parts of the longitudinal (xx, solid line) and Hall (xy, dashed line) dynamical conductivities; Kerr angle (c) and reflectivity (d). The magnetic field $B = 7$ T; the temperature $T = 0.1$ meV is less than the level broadening $\Gamma = 3.5$ meV.

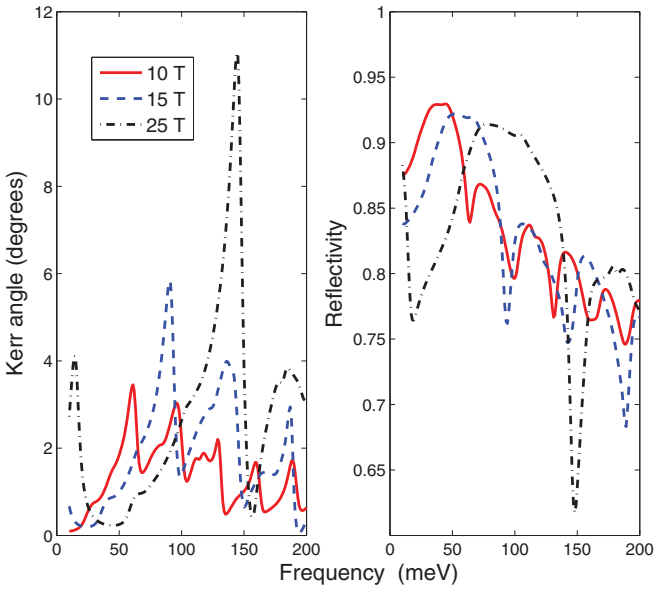

FIG. 4. (Color online) Kerr angle and reflectivity at 10, 15, and 25 T.

(90 meV) near the K point. Besides, the transitions $|11\rangle \rightarrow |10\rangle$ (95 meV) near the H point make a contribution as well. All these lines obeying the selection rule $\Delta n = 1$ are strong. There are two weak lines in the frequency range. One ($|24\rangle \rightarrow |32\rangle$) is seen at 55 meV as a shoulder on the theoretical curve. Another, at 31 meV, results from the transitions $|10\rangle \rightarrow |32\rangle$ near the K point.

The positions of the lines for fields in the range of 10–30 T agree with observations of Refs. 8 and 18.

The optical Hall conductivity $\sigma_{xy}(\omega)$ in the ac regime is shown in Figs. 3(a) and 3(b). The conductivities $\sigma_{xx}(\omega)$ and $\sigma_{xy}(\omega)$ allow us to calculate the Kerr rotation and the reflectivity as functions of frequency [see Figs. 3(c) and 3(d)]. It is evident that the interpretation of the Kerr rotation governed by the conductivity $\sigma_{xy}(\omega)$ is much more complicated in comparison with the longitudinal conductivity.

The Kerr angle and reflectivity shown in Fig. 4 for the different magnetic fields demonstrate the strong field dependence of the magneto-optic phenomena.

V. SUMMARY AND CONCLUSIONS

In conclusions, we have evaluated the perturbation theory for the matrix Hamiltonian, which permits one to calculate the corrections to the eigenvalues resulting from the small matrix elements particularly from the trigonal warping. We have shown that the trigonal warping in graphite can be considered within the perturbation theory at strong magnetic fields larger than approximately 1 T. We have found that the main optical transitions obey the selection rule $\Delta n = 1$ for the Landau number n, however, the $\Delta n = 2$ transitions due to the trigonal warping with small probability are also essential. Good agreement between the calculations and the measured Kerr rotation and reflectivity in graphite in the quantizing magnetic fields is achieved. The SWMC model parameters are used in the fit taking into account the previous dHvA measurements and correcting the Fermi energy for the case of strong magnetic fields.

ACKNOWLEDGMENTS

The author is thankful to A. Kuzmenko and J. Levallois for useful discussions and for communicating their experimental results prior to publication. This work was supported by the Russian Foundation for Basic Research (Grant No. 10-02-00193-a) and by the SCOPES Grant No. IZ73Z0_128026 of the Swiss National Science Foundation. The author is grateful to the Max Planck Institute for Physics of Complex Systems for its hospitality in Dresden.

[1] J. W. McClure, Phys. Rev. **108**, 612 (1957); J. C. Slonczewski and P. R. Weiss, *ibid.* **109**, 272 (1958).
[2] H. Suematsu and S-i. Tanuma, J. Phys. Soc. Jpn. **33**, 1619 (1972).
[3] W. W. Toy, M. S. Dresselhaus, and G. Dresselhaus, Phys. Rev. B **15**, 4077 (1977).
[4] R. E. Doezema, W. R. Datars, H. Schaber, and A. Van Schyndel, Phys. Rev. B **19**, 4224 (1979).
[5] E. Mendez, A. Misu, and M. S. Dresselhaus, Phys. Rev. B **21**, 827 (1980).
[6] Z. Q. Li, S.-W. Tsai, W. J. Padilla, S. V. Dordevic, K. S. Burch, Y. J. Wang, and D. N. Basov, Phys. Rev. B **74**, 195404 (2006).
[7] M. Orlita, C. Faugeras, G. Martinez, D. K. Maude, M. L. Sadowski, and M. Potemski, Phys. Rev. Lett. **100**, 136403 (2008).
[8] M. Orlita, C. Faugeras, J. M. Schneider, G. Martinez, D. K. Maude, and M. Potemski, Phys. Rev. Lett. **102**, 166401 (2009).
[9] M. Orlita and M. Potemski, Semicond. Sci. Technol. **25**, 063001 (2010).
[10] I. Crassee, J. Levallois, A. L. Walter, M. Ostler, A. Bostwick, E. Rotenberg, T. Seyler, D. van der Marel, and A. Kuzmenko, Nature Physics **7**, 48 (2011).
[11] Y. Kopelevich, J. H. S. Torres, R. R. da Silva, F. Mrowka, H. Kempa, and P. Esquinazi, Phys. Rev. Lett. **90**, 156402 (2003).
[12] I. A. Luk'yanchuk and Y. Kopelevich, Phys. Rev. Lett. **97**, 256801 (2006).
[13] Z. Jiang, Y. Zhang, H. L. Stormer, and P. Kim, Phys. Rev. Lett. **99**, 106802 (2007).
[14] J. M. Schneider, M. Orlita, M. Potemski, and D. K. Maude, Phys. Rev. Lett. **102**, 166403 (2009).
[15] A. N. Ramanayaka and R. G. Mani, Phys. Rev. B **82**, 165327 (2010).
[16] L. A. Falkovsky, Phys. Rev. B **82**, 073103 (2010).
[17] G. Li and E. Y. Andrei, Nature Phys. **3**, 623 (2007).
[18] K.-C. Chuang, A. M. R. Baker, and R. J. Nicholas, Phys. Rev. B **80**, 161410(R) (2009).
[19] L. M. Zhang, Z. Q. Li, D. N. Basov, M. M. Fogler, Z. Hao, and M. C. Martin, Phys. Rev. B **78**, 235408 (2008).

[20]H. Ushio, T. Uda, and Y. Uemura, J. Phys. Soc. Jpn. **33**, 1551 (1972).
[21]K. Nakao, J. Phys. Soc. Jpn. **40**, 761 (1976).
[22]B. Partoens and F. M. Peeters, Phys. Rev. B **74**, 075404 (2006).
[23]A. Grüneis, C. Attaccalite, L. Wirtz, H. Shiozawa, R. Saito, T. Pichler, and A. Rubio, Phys. Rev. B **78**, 205425 (2008).
[24]A. B. Kuzmenko, I. Crassee, D. van der Marel, P. Blake, and K. S. Novoselov, Phys. Rev. B **80**, 165406 (2009).
[25]G. Dresselhaus, Phys. Rev. B **10**, 3602 (1974).
[26]W.-K. Tse and A. H. MacDonald, Phys. Rev. B **82**, 161104(R) (2010).
[27]T. Morimoto, Y. Hatsugai, and H. Aoki, Phys. Rev. Lett. **103**, 116803 (2009).
[28]A. A. Abrikosov, L. P. Gorkov, and I. E. Dzyaloshinski, *Methods of Quantum Field Theory in Statistical Physics* (2ed, Pergamon, 1965).
[29]L. A. Falkovsky and A. A. Varlamov, Eur. Phys. J. B **56**, 281 (2007).
[30]A. B. Kuzmenko, E. van Heumen, F. Carbone, and D. van der Marel, Phys. Rev. Lett. **100**, 117401 (2008).
[31]N. B. Brandt, S. M. Chudinov, and Ya. G. Ponomarev, *Semimetals I. Graphite and Its Compaunds* (Elsevier, Amsterdam, 1988).